Optical Spectroscopy, Electron Spin, and Radioactive Decay

Duncan Beauch with Charlotte Hoelzl

April 5, 2022

Introduction

Nuclear physics can oftentimes appear to be a puzzling area of physics as unusual phenomena occur on scales and frequencies that we are unable to observe with the naked eye. In the following experiments we will perform experiments that can be seen with the naked eye and perform calculations to determine their source.

First, we will explore optical spectroscopy and use Bragg's Law, Rydeberg constant, and the Balmer Series to determine wavelengths of light, ionization potential of atoms, and spacings between microscopic gratings.

Next, we will observe the quantum spin property of electrons and manipulate samples of diphenyl-picryl-hydrazil (DPPH) salt using magnetic fields to determine the g-factor of a free electron. This g-factor allows us to relate the magnetic moment and angular momentum of the electron

Finally, we will observe the radioactive decay of various isotopes using a diffusion cloud chamber and Geiger-Müller Counter. We will then use our data to find the energy of alpha radiation and find statistical means to predict the decay rate of beta particles.

Experiment 1: Atomic Spectra

In the following set of spectroscopic procedures, we will be using a grating spectrometer table as shown in Figure 1 with a grating rated to be 600 lines/mm.

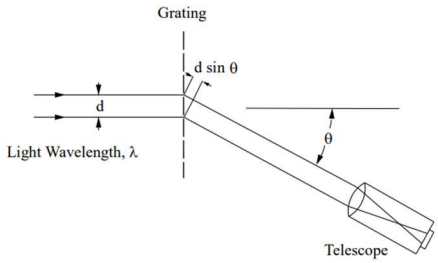

Figure 1: Grating spectrometer table with attached telescope

On the opposite side of the grating from the telescope we will place various light sources and view their optical spectra to determine values for the grating spacing, wavelength of spectral lines, and Rydeberg constant. The telescope is focused for parallel light and collimator slit adjusted to the focal point of the lens.

First, we will use a sodium lamp as our light source and through the telescope two bright yellow spectral lines are observed corresponding to the spin up and spin down energy transitions produced by the sodium lamp. Using these two lines we can measure the angle between them and calculate the grating spacing d as follows:

$$d = \frac{m\lambda}{sin\theta}$$

Here m is the diffraction order and λ is the wavelength of the sodium spectra known to be $\lambda = 589.0$ nm. The angle between lines was measured several times and the average value was used to achieve a more accurate measurement for such a small measurement. Using an angle of 20.89°, the grating constant was calculated to be $d =$ 605 ± 1 lines/mm.

Similarly, we can find the difference in wavelength between the two spectral lines $\Delta\lambda$ by measuring the difference in angle $\Delta\theta$:

$$\Delta\lambda = \frac{d * \cos(\theta) * \Delta\theta}{m}$$

This is done for the second order spectra and a value for the difference in wavelength was calculated as $\Delta\lambda = 0.6 \pm 0.1°$. This is exactly the theoretical value, however, there is quite a large error in the calculation as the mechanical tools used have trouble in the smaller range of measure.

Next, we will replace the sodium lamp with a power supply with interchangeable spectrum tubes. We will start with hydrogen in order to measure the Rydeberg constant which is known to a very precise value.

For hydrogen there are four visible spectra of violet, blue, blue-green, and red in both the first and second order. We can calculate the Rydeberg constant R_H using the equation:

$$\frac{1}{\lambda} = R_H\left(\frac{1}{{n_f}^2} - \frac{1}{{n_i}^2}\right)$$

Where n_f and n_i represent the final and initial states of the hydrogen. In our case, we know that the final state of the spectra is the $n_f = 2$ state, and we can find the initial state using the Balmer formula. Using this data, we can plot $\frac{1}{\lambda}$ vs. $\left(\frac{1}{{n_f}^2} - \frac{1}{{n_i}^2}\right)$ to obtain the plot shown in Figure 2 whose slope is our estimate for the Rydeberg constant. This was done for all four lines in the first order as well as the red and blue-green spectra of the second order.

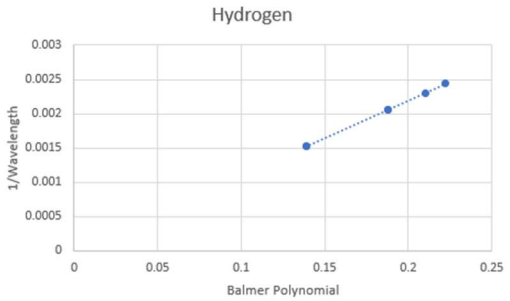

Figure 2: Plot for hydrogen spectral lines to find the Rydeberg constant

The Rydeberg constant was found to be $R = 1.09646 \pm 0.032 \times 10^7\ m^{-1}$. The spectral lines that we have observed originate from the transitions which end at the $n = 2$ state as shown circled in Figure 3.

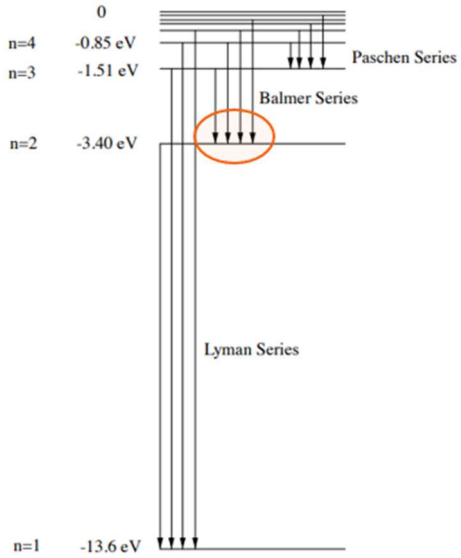

Figure 3: Hydrogen energy level diagram with relevant transition circled in orange

Now we can calculate the ionization potential of hydrogen using the following equation:

$$E = hcR_H = 13.595\ eV$$

The same procedure will now be performed with a helium spectrum tube. Six distinct spectral lines can be seen of red, orange, green, blue-green, blue, and violet. Their angles are measured, and wavelengths calculated as follows with the blue line as an example:

$$\lambda_{blue} = \frac{d * \sin(\theta)}{m} = 471.7\ nm$$

This line is unique because it corresponds to the helium as it loses its electron entirely and ionizes. Using this fact, we can determine the final and initial energy states of the helium for this transition to occur using a similar equation as for hydrogen, modified for the helium atom:

$$\frac{1}{\lambda} = Z^2 R_\infty \left(\frac{1}{{n_f}^2} - \frac{1}{{n_i}^2}\right)$$

Where Z represents the atomic number of the atom, in the case of helium $Z = 2$. We find that the transition which produces the blue spectral line comes from an initial state of $n_i = 5$ to a final state of $n_f = 2$.

Now we replace the helium spectrum tube with a neon spectrum tube. We can attempt to prove our understanding of atomic spectra by predicting the angle of a given wavelength. The line corresponding to a transition from the 5s to 3p levels has a known wavelength of $\lambda = 632.8$ nm. Using our equation from before we can calculate the expected angle to be $\theta = 22.49°$. Checking experimentally, we find the spectral line at about $\theta = 23.416 \pm 0.1°$.

Experiment 2: Electron Diffraction

Now that we have proven our understanding of the diffraction of light, we can expand this idea to matter waves, specifically electron waves. To do this we will use the apparatus shown in Figure 4.

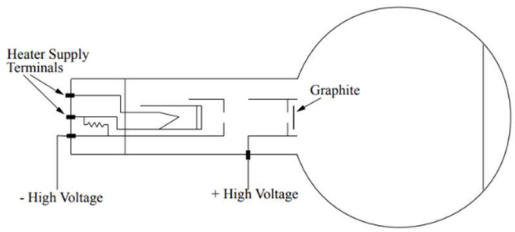

Figure 4: Electron diffraction apparatus

We can calculate the space between graphite crystals using the relationship:

$$D = \frac{2nLh}{d\sqrt{2em_e}} * \frac{1}{\sqrt{V}}$$

Where D is the measured diameter of the rings produced and V is the supplied voltage to the apparatus. The voltage supply was swept over 2 V and 4.4 V at 0.4 V increments and the diameter of the first two rings was recorded. Using known values for the other constants we can plot D vs $\frac{1}{\sqrt{V}}$ to find the spacing d. This plot is shown in Figure 5.

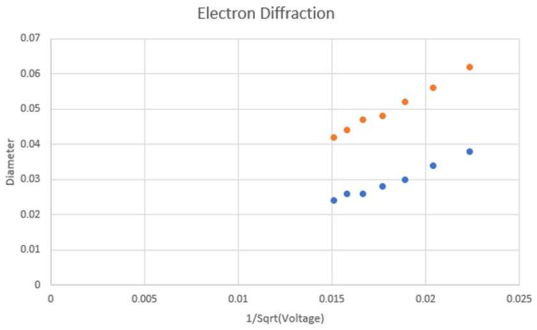

Figure 5: Plot of diameter vs. 1/sqrt(voltage) for the electron diffraction apparatus

The two spacings are then calculated to be $d = 174.3 \pm 1.2$ pm and $d = 246.1 \pm 9.5$ pm which are very close to the expected values.

Experiment 3: Electron Spin Resonance

In this experiment we will explore the g-factor of an electron, the quantity which characterizes its magnetic moment and angular momentum. In a completely free electron this g-factor is 2. However, it is difficult for us to properly trap a set of electrons and measure their transitions accurately so we will substitute this for the salt molecule DPPH which happens to have a characteristic g-factor of roughly 2. Our goal will be to measure this g-factor by

inducing spin transitions of the molecule through a radio-frequency magnetic field and separate the two levels with a static magnetic field. The setup for this experiment is shown in Figure 6.

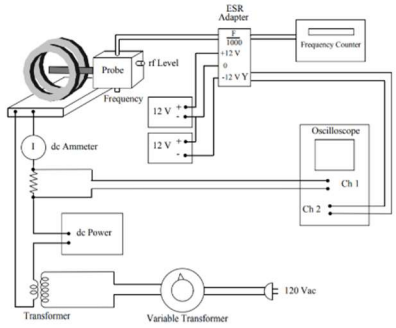

Figure 6: g-factor experiment with ESR circuit, DPPH probe, and Helmholtz coils

The probe containing the DPPH sample is placed in the center of a set of Helmholtz coils which produce our static magnetic field of $B \approx 0.779$ mT/A. However, we want to see the system at resonance, so to contextualize the frequency of oscillation we superimpose a 60 Hz AC current as shown in Figure 6.

With the spin frequency connected to the oscilloscope we are able to see the response of the DPPH sample to a change in magnetic field strength by varying the supplied current. Resonance was observed at a current $I = 3.56$ A and corresponding magnetic field calculated as follows:

$$B_z = \frac{8}{\sqrt{125}}\frac{\mu_0 NI}{R} = 2.8\,mT$$

This experiment is affected on some level by the Earth's magnetic field, however, since its contribution is on the scale of μT, it is negligible.

This process was repeated in increments of 10 MHz down to 23 MHz where the resonant frequency f and current I were recorded to create the plot of I vs. f shown in Figure 7.

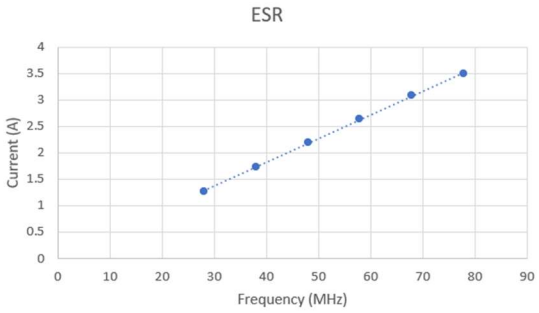

Figure 7: Current vs. resonant frequency for the electron spin apparatus

Using the equations shown below, we can calculate the g-factor of DPPH as follows:

$$I = f\frac{\sqrt{125}Rh}{8g\mu_0 N\mu_B}$$

$$g = \frac{\sqrt{125}Rh}{8(slope)\mu_0 N\mu_B}$$

Using our experimental data with a slope = 0.0448, we can calculate a factor $g = 2.046 \pm 0.022$. This is quite close to the known g-factor of a DPPH electron $g = 2.0036$.

Experiment 4: Diffusion Cloud Chamber

In this experiment, we will use a diffusion cloud chamber to watch the alpha and beta decay of radioactive materials. The setup consists of a pot with a clear glass lid and stopper in the middle. The inside edges are covered with paper that are soaked in isopropyl alcohol and the base is cooled by a pump using ice water. This creates an atmosphere inside the pot in which super-saturated alcohol vapor forms a layer a few centimeters from the bottom of the pot. LEDs line the edges illuminating the vapor particles which can be seen with the naked eye inside. The setup is depicted in Figure 8.

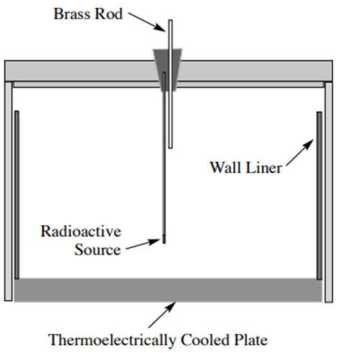

Figure 8: Diffusion cloud chamber

Our first radioactive source is a sample of Polonium-210 which produces mainly alpha particles that appear as long trails of ionized alcohol passing through the vapor layer. To measure the true length of one of these trails we want to observe a near instantaneous burst from the source as that means an alpha particle was shot out from the source in a completely horizontal direction which passes through the visible vapor layer parallel. One such decay was observed, and the length was estimated to be about 3.75cm. This corresponds to an energy of between 5 and 6 MeV which is as expected with the theoretical value of 5.305 MeV.

For comparison we replace the Polonium-210 sample with a sample of Strontium-90. Unlike polonium, this isotope decays majorly by beta decay. These particles appear in the diffusion chamber much different than alpha particles as they do not travel in straight lines and leave much shorter and fainter tracks than alpha particles.

Replacing the Strontium-90 sample with just a rubber stopper we can observe ambient background radiation. There are many tracks that still appear in the vapor without a large radioactive source present. These are mostly due to cosmic rays and radiation from materials all around including materials like the building itself.

Experiment 5: Statistics of Radioactive Decay

In this experiment we will continue to observe the decay of radioactive isotopes. Our radioactive source consists of a sample of Cesium-137 which we will observe using a Geiger-Müller Counter (GM) to detect the beta particles it releases. Although radioactive decay is characteristically random, we are able to predict its behavior over a long period of time using statistics.

First, we will observe the decay for a small decay rate ~2 counts per second. The GM Counter sends its output to our Capstone program which records the decay rate in one second intervals. After running the experiment for 5 minutes, we obtain 300 samples of the decay rate which can be used to compare with statistical models. This experiment yielded a mean of 1.43 decays per second and the data is shown in Figure 9 along with a theoretical model of the Poisson and Gaussian distributions with equivalent mean and standard deviations.

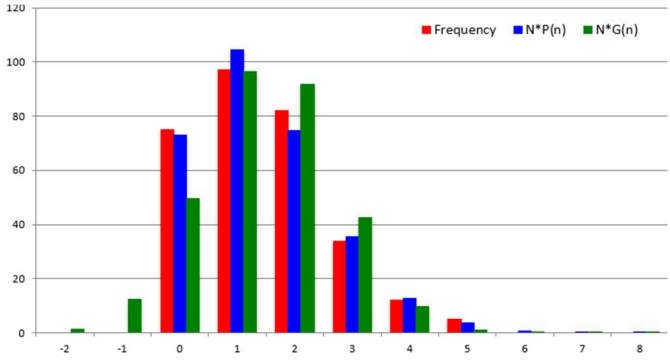

Figure 9: Beta decay rate of Cs-137 at a low decay rate compared with Poisson and Gaussian distributions

Clearly the Poisson distribution (blue) matches the data (red) better than the Gaussian distribution which is as expected.

However, for larger mean decay rates ~40 decays per second this does not hold. The same experiment was done with a larger decay rate by moving the Cesium-137 sample closer to the GM Counter. This experiment yielded a mean of 36.19 decays per second and the data is shown in Figure 10 along with the theoretical models with equivalent mean and standard deviations.

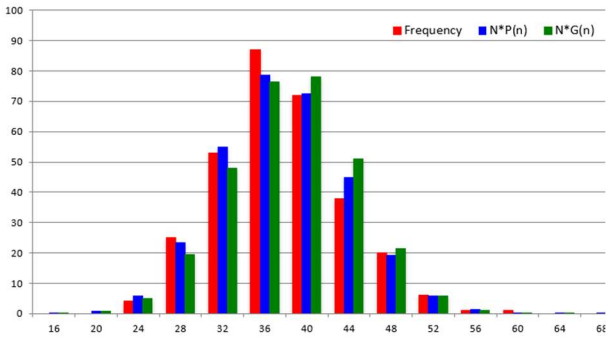

Figure 10: Beta decay rate of Cs-137 at a high decay rate compared with Poisson and Gaussian distributions

In this case the Gaussian distribution (green) appears to be a better fit for the data. This trend will theoretically become more apparent with larger decay rates as the rate of decay tends towards infinity.

Conclusion

In experiment 1, we proved Bragg's Law through various means in which we were able to calculate the grating constant, wavelength of light, or angle of diffraction given the other two parameters. We used this in conjunction with the Rydeberg constant to calculate the ionization energy of hydrogen which was within 1% of the theoretical value and reversed the process to find the Rydeberg constant to also 1% of the theoretical value. We then used this relationship to determine the initial and final energy states of the helium atom for a specific spectral emission.

In experiment 2, we extended this proof and procedure to the electron diffraction apparatus in which we proved the laws hold for matter waves as well as light. This allowed us to measure the spacing between the structure of a graphite crystal on the scale of picometers.

In experiment 3, we manipulated magnetic fields to show how electrons flip between spin up and spin down and that this oscillation has a resonance known as electron spin resonance. This was used to determine the g-factor of an electron-like molecule DPPH where we calculated the value to within 2% of the theoretical value.

In experiment 4, we created a visualization for the emission of alpha and beta particles from radioactive sources. Our diffusion chamber allowed us to make a somewhat crude estimate for the energy of the emitted alpha particles by measuring their ionization trails. We also showed that radiation is all around us in the form of cosmic rays and ambient radiation from our environment.

In experiment 5, we proved that although individual radioactive decays are characteristically random, the rate of decay is not and can be modeled using statistical techniques. Using GM Counters, we recorded data that shows how smaller rates of decay are modeled by Poisson statistics whereas larger decay rates are best modeled by Gaussian statistics.